

## **THERMAL BEHAVIOUR OF DICKITE-DIMETHYL-SULFOXIDE INTERCALATION COMPLEX**

*F. Franco\* and M. D. Ruiz Cruz*

Departamento de Química Inorgánica, Cristalografía y Mineralogía Facultad de Ciencias, Campus de Teatinos Universidad de Málaga 29071, Málaga, Spain

(Received November 5, 2002; in revised form April 9, 2003)

### **Abstract**

The thermal behaviour of the intercalation complex of a dickite from Tarifa, Spain, with dimethylsulfoxide was studied by high-temperature X-ray diffraction, differential thermal analysis and thermogravimetry, and attenuated total reflectance infrared spectroscopy. The ATR-FTIR study indicated that the heating between room temperature and 75°C produced the elimination of adsorbed molecules. Above this temperature the elimination of intercalated molecules occurs through several stages. Loss of ~6.5% of the intercalated DMSO first causes a slight contraction of the basal spacing at 90°C due to a rearrangement of the DMSO molecules in the interlayers positions. This contraction is followed by the formation of a single layer complex and the restoring of the dickite structure, at 300°C, when the loss of intercalated species have been completed.

**Keywords:** ATR-FTIR, dickite, dimethylsulfoxide, DTA-TG, HTXRD, intercalation complex, kaolinite

### **Introduction**

Dickite, like the other kaolin polytypes, kaolinite and nacrite, can react with both organic and inorganic materials to form intercalation complexes. The reactive guest molecules enter the interlayer space and expand the dickite layers, breaking the bonds between the dickite hydroxyl groups and the oxygens of the adjacent siloxane sheet. Then, the intercalated molecules form hydrogen bonds with either the siloxane or the hydroxyl surface of the kaolin mineral [1]

Kaolinite-DMSO intercalation complex (K-DMSO) has been extensively studied by X-ray diffraction, spectroscopic and thermoanalytical methods [1–11]. On the other hand, the dickite-DMSO intercalation complex (D-DMSO) has been studied by X-ray diffraction and spectroscopic methods [1, 4, 12] and there is no information about its thermal behaviour.

\* Author for correspondence: E-mail: ffranco@uma.es

A structural model of the K-DMSO complex was proposed by Thompson and Cuff [7] using spectroscopic and X-ray and neutron powder diffraction data. In this structure, each DMSO molecule is hydrogen bonded to three inner-surface hydroxyl groups above the octahedral vacancy in the gibbsitic sheet of the kaolinite layer. One methyl group, with its S–C bond, is keyed into the ditrigonal hole in the tetrahedral sheet and the other S–C bond is parallel to the sheet. The accommodation of the DMSO molecules causes a significant horizontal displacement of the individual layers to achieve almost perfect overlap of the octahedral vacancy by the adjacent ditrigonal holes.

Recently, based on Raman spectroscopic results, Frost *et al.* [8, 10] undertook a molecular structural study of the K-DMSO complex and proposed a model in which water and DMSO are intercalated. Two types of DMSO, monomeric and polymeric, are present in the intercalate in such a way that every inner-surface hydroxyl group is individually hydrogen bonded to one DMSO molecule. Water was considered to be essential to the intercalation process and serves as the linkage molecule in the polymeric DMSO.

Franco and Ruiz Cruz [11], using high-temperature X-ray diffraction (HTXRD), differential thermal analysis (DTA) and thermogravimetry (TG) showed that heating of the K-DMSO complex between 25–300°C caused the removal of the DMSO, which occurred through several stages. In the first stage (between 25–50°C), a slight increase in the intensity of the complex reflections revealed a better packing of the complex caused by the loss of adsorbed molecules (water+DMSO). The mass loss in this first stage represented ~3.74% of the initial mass. In a second stage, heating between 50 and 125°C led to an expansion (from 11.19 to 11.28 Å) followed by a contraction (from 11.28 to 11.19 Å) at the same time that the intensity of the basal reflection decreased and was replaced by a broad band extending from ~11 to ~7 Å. At the end of this stage the  $[\text{Si}_2\text{Al}_2\text{O}_5(\text{OH})_4]:[(\text{CH}_3)_2\text{SO}]$  ratio was close to 1:0.9. In a third stage (between 125–200°C), the loss of DMSO did not cause changes in the HTXRD patterns; and finally, in a fourth stage (between 200–300°C), a new loss of DMSO caused a significant increase in intensity and sharpening of the basal reflection of kaolinite.

Although D-DMSO intercalation complex has already been studied by X-ray diffraction and FTIR spectrometry [1, 4, 12] more detailed investigations are necessary to determine the differences in thermal behaviour among the DMSO intercalation complexes formed from the several kaolin polytypes. In this sense, the application of high-temperature X-ray diffraction (HTXRD) to the study of intercalated kaolins has proven to be very useful. For example, HTXRD was used to determine the thermal behaviour of the kaolinite-hydrazine and the dickite-hydrazine intercalation complexes [13, 14].

The present paper forms part of a wider investigation that includes the study of the thermal behaviour of several kaolin–mineral intercalation complexes. We report here the results of the study of the thermal behaviour of D-DMSO with the aim of completing the previous study of the K-DMSO complex.

## Experimental

The specimen used for this study was a dickite from Tarifa, Spain. At the sampling locality, dickite fills veins as the only constituent or occurs along with kaolinite [15]. The selected sample consisted of dickite alone and no other impurities were detected by XRD. Dickite occurs either as stacks of particles 5–10  $\mu\text{m}$  thick or as blocky crystal with similar sizes. The reagent used was 98% pure dimethyl-sulfoxide (PANREAC, Montplet & Esteban, Barcelona and Madrid, España). The D-DMSO intercalation complex was obtained by placing an oriented sample of dickite in a DMSO-atmosphere, at 50°C and increasing time intervals. Natural dickite was characterized by X-ray diffraction (XRD), differential thermal analysis (DTA), thermogravimetry (TG) and by attenuated total reflectance infrared spectrometry (ATR-FTIR). The D-DMSO intercalate was studied using high-temperature X-ray diffraction (HTXRD), DTA-TG and ATR-FTIR.

The DMSO-treated sample was spread on the platinum (Pt) holder of a Siemens D-5000 diffractometer. The HTXRD patterns were obtained using  $\text{CuK}\alpha$  radiation at 40 kV and 30 mA, a  $2\theta$  step size of  $0.02^\circ$  and a counting time of 1 s. The heating rate was  $4^\circ\text{C s}^{-1}$ . The samples were heated to a particular temperature and held there for 600 s prior to the acquisition of the XRD pattern. Diffractograms were obtained after variable temperature intervals (between 5–50°C) according to the expected modifications indicated by the DTA-TG curves. The Pt reflection at 2.28 Å was used as a standard for the accurate determination of the  $d$  values.

Thermal analyses were performed in a Setaram thermal analyser equipped with a CS32 controller.  $\text{Al}_2\text{O}_3$  was used as reference material. 20 mg of sample was used in both natural dickite and D-DMSO complex analysis. DTA and TG curves were recorded simultaneously in static air at a heating rate of  $10^\circ\text{C min}^{-1}$ .

Attenuated total reflectance (ATR-FTIR) spectra of the powdered samples were obtained with a Golden Gate single reflection ATR apparatus from SPECAC fitted with a FTIR spectrometer Bruker Equinox 55. 300 scans were averaged in each case to optimise the signal-to-noise ratio. The samples were previously heated to a particular temperature and held at this temperature for 600 s before their placement in the spectrometer. The intensity of the Si–O bands was used to normalize the ATR-FTIR spectra.

Baseline adjustment and band component analysis of both the ATD curves and ATR-FTIR spectra were carried out using the peakfit software from Jandel Scientific. Lorentz–Gauss cross product functions were used throughout and peak fitting was carried out until correlation coefficients with  $r^2 > 0.997$  were obtained.

## Results

### *X-ray diffraction study*

Intercalation of DMSO into dickite caused the expansion from a basal spacing of 7.15 to 11.04 Å (Fig. 1a). This basal spacing is similar to the 11.19 Å spacing observed af-

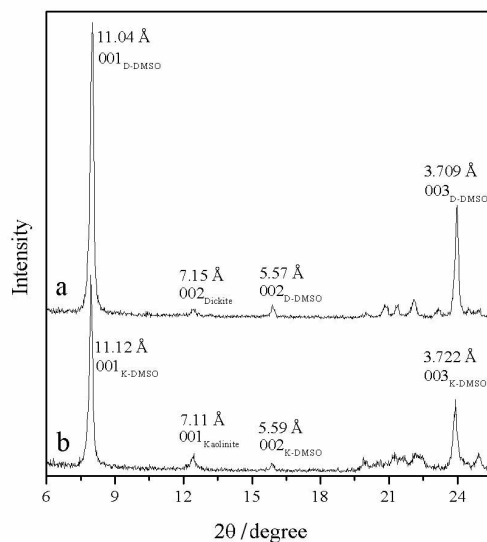


**Fig. 1** X-ray diffraction pattern of a – dickite-DMSO complex and b – kaolinite-DMSO complex, both obtained at room temperature from orientated samples

ter intercalation of kaolinite [11] (Fig. 1b). The obtained complex displays a sharp 001 reflection as well as weaker higher-order 001 reflections. The patterns also show the presence of non-basal reflections in the  $18\text{--}23^\circ$   $2\theta$  zone of the diagrams which are better defined than the reflections shown by the K-DMSO complex (Fig. 1b). The degree of intercalation (*I.R.*) was estimated as a relation between the integrated areas of the 002 reflection of the non-intercalated dickite at  $25^\circ\text{C}$  and after heating at  $300^\circ\text{C}$ , when dickite has been completely deintercalated.

$$I.R. = 100 \frac{I_{(002)\text{dickite}}^{300^\circ\text{C}} - I_{(002)\text{dickite}}^{25^\circ\text{C}}}{I_{(002)\text{dickite}}^{300^\circ\text{C}}}$$

This new method for determination of the degree of intercalation, which is not dependent on the intensity of the complex reflections, is proposed by Franco and Ruiz Cruz in a work which is actually submitted. This method is based on the assumption that both the deintercalated and the non-intercalated fraction of dickite show similar intensity of the basal reflections.

Four weeks of treatment were necessary to achieve a degree of intercalation (90%) similar to that (92%) measured in the complex formed with kaolinite after three days of treatment [11]. This different intercalation rate can be attributed to the notably larger particle size of dickite ( $5\text{--}10 \mu\text{m}$ ) compared to that of kaolinite ( $<0.2 \mu\text{m}$ ).

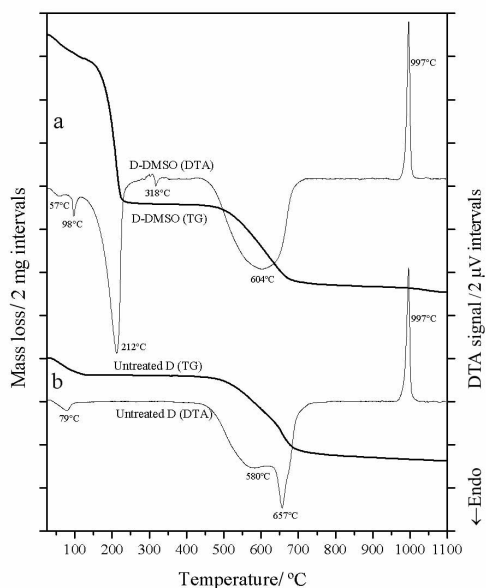


**Fig. 2** DTA-TG curves of a – the dickite-DMSO intercalation complex and b – untreated dickite

#### *DTA-TG study*

The DTA-TG curves of the D-DMSO complex and the untreated dickite are shown in Fig. 2. Heating of the complex at a continuous rate causes an intense mass loss between room temperature and 300°C, which is accompanied by three endothermic effects: Two weak effects are centred at 57 and 98°C; a third (more intense) occurs at about 212°C. The first represents a mass loss about 8% of the total loss below 300°C. The mass loss associated with the second endothermic effect is about 6% of the loss below 300°C. The third endothermic effect correlates with a faster mass loss, which represents about 86% of the total below 300°C. Assuming that the first mass loss (below 75°C) corresponds to the loss of adsorbed molecules as deduced from ATR-FTIR spectra, the TG curve permits an estimate of the ratio  $[\text{Si}_2\text{Al}_2\text{O}_5(\text{OH})_4]:[(\text{CH}_3)_2\text{SO}]$  in interlayer positions of about 1:0.88, at 75°C. This ratio becomes 1:0.82 at the beginning of the third mass loss stage (at 125°C). Taking into account that the intercalation degree estimated from XRD measurements is 90% the ratio  $[\text{Si}_2\text{Al}_2\text{O}_5(\text{OH})_4]:[(\text{CH}_3)_2\text{SO}]$  in the intercalated fraction is nearly to 1:1.

The low-temperature endothermic effects are almost immediately followed by a weak exothermic effect at 318°C, similar to those observed in the DTA curve of the kaolinite-DMSO complex [11], which probably corresponds to a rearrangement of the dickite layers.

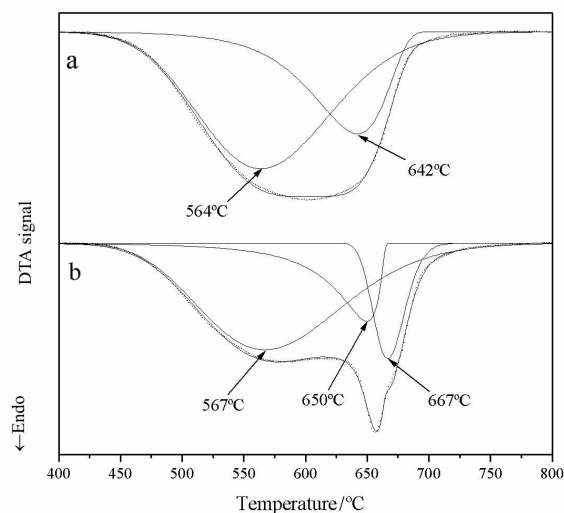


**Fig. 3** Band component analysis of the DTA curves of a – dickite-DMSO complex and b – untreated dickite in the range 400–800°C

The wide endothermic effect centred at 604°C corresponds to the dehydroxylation of dickite (Fig. 2a). This effect appears notably modified in relation with those observed in the untreated dickite (Fig. 2b). In the untreated dickite (Fig. 2b), dehydroxylation yields two overlapping endothermic effects centred at 580 and 657°C. According to Frost and Vasallo [16] and Stoch [17], these endothermic effects can be assigned as follows: the endothermic at 580°C due to the loss of the inner-surface hydroxyls and the endothermic effects at 657°C due to the loss of the inner hydroxyls. The band component analysis of this complex endothermic effect (Fig. 3b) shows that the 657°C effect represents the sum of two peaks centred at 650 and 667°C. The interpretation of these two endothermic effects is difficult with the results presented in this work, but they seem to indicate that dehydroxylation of the inner hydroxyls takes place in two steps. Nevertheless, a major detailed investigation is necessary to offer more reliable conclusions. On the other hand, the fitting of the endothermic effect observed, between 400 and 700°C, in the DTA curve of the D-DMSO complex appears to be formed by only two effects at 564 and 642°C (Fig. 3a). These effects occur at lower temperatures and in a narrower range of temperatures compared to that observed in the untreated dickite.

#### *HTXRD study*

The HTXRD patterns obtained at increasing temperatures are shown in Fig. 4, and the intensities of the first basal reflection of the D-DMSO complex and the 7-Å reflection of dickite vs. temperature are plotted in Fig. 5. This latter is a basal reflection of dickite and provide information about the unreacted fraction of dickite, at room

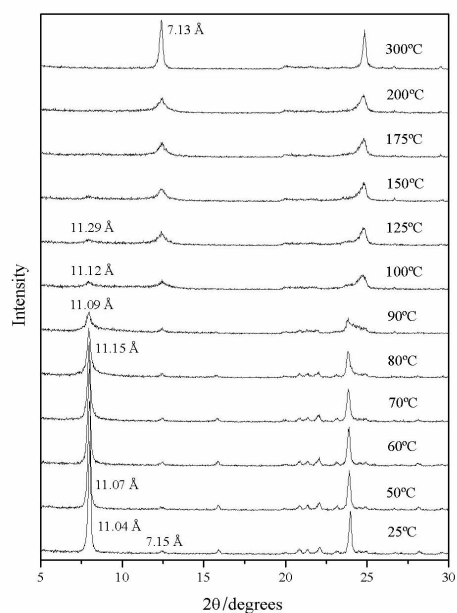


**Fig. 4** HTXRD patterns of the dickite-DMSO complex obtained after heating in the range 25–300°C

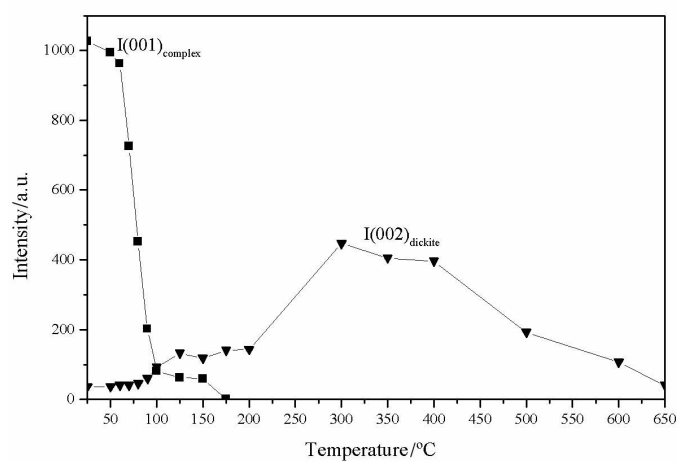


**Fig. 5** Variation of the intensity of the basal reflection of the dickite-DMSO complex (full square) and dickite (full triangle) in the temperature range of 25–650°C

temperature, and about the reorganization of deintercalated dickite layers at higher temperatures. The HTXRD patterns permitted the distinction of four main stages of removal of the intercalated molecules:

1) In the first stage (below 90°C) the partial removal of the DMSO causes a gradual decrease in intensity of the complex reflections, which is more evident for the 001 and 003 reflections (Figs 4 and 5). This intensity decrease is not accompanied by a similar increase in the intensity of the non-intercalated dickite reflections. Moreover, a slight dilation of the structure perpendicularly to the layers (from 11.04 to 11.15 Å) is observed between room temperature and 80°C.

2) In a second stage, between 90 and 125°C (Figs 4 and 5), a slower diminution of the 001 complex reflection is accompanied by a slow increase of the 7-Å dickite reflection. A small contraction of the basal spacing (from 11.15 to 11.09 Å) occurred at 90°C. From this temperature, the loss of definition of the non-basal reflections (between 20 and 23° 2 $\theta$ ) indicates the loss of the three-dimensional ordering.

3) Between 125 and 200°C (Figs 4 and 5), the decrease and the later disappearance of the 001 basal reflection of the 11-Å complex is not accompanied by an increase in intensity of the dickite reflections.

4) Finally, above 200°C an increase in intensity of the dickite reflections is observed, which indicates the structural rearrangement of the deintercalated dickite layers (Figs 4 and 5). Nevertheless, the XRD patterns of the deintercalated dickite show some differences with regard to that of the untreated dickite. Although the number of layers in the diffracting domain of the D-DMSO complex, calculated using the Scherrer equation [18], is similar (68) to that observed in untreated dickite (73), the decreasing of the HI (Hinckley index) adapted to dickite [19] (from 2.24 to 1.00) indicates that the intercalation of DMSO molecules in the interlayer space of dickite and the later deintercalation caused an increase in disorder.

The drastic decrease in intensity of the dickite reflection above 400°C (Fig. 5) indicates the beginning of the dehydroxylation process. This is also in accordance with the DTA-TG results (Fig. 2), which reveals that the endothermic effect due to dehydroxylation begins at 450°C.

#### *ATR-FTIR study*

To ensure the correct interpretation of the different stages of mass loss observed in the DTA-TG analysis, ATR-FTIR spectra were obtained at specific temperatures. The spectra were obtained at room temperature and after heating at 75, 115, 175 and 350°C. The OH-stretching region of the ATR-FTIR spectra of the untreated dickite, the D-DMSO intercalation complex obtained at room temperature and the D-DMSO complex heated at higher temperatures are shown in Fig. 6. The ATR-FTIR spectrum of the untreated dickite shows the three characteristic bands in the  $\nu$ OH region at 3700, 3644 and 3619  $\text{cm}^{-1}$ , designed as 1, 2 and 3, respectively. These bands were assigned by Farmer [20] to the inner-surface hydroxyl groups (bands 1 and 2) and to the inner hydroxyl group (band 3).

A comparison between the infrared spectra of the untreated dickite and the dickite-DMSO intercalation complex shows that intercalation causes a strong decrease in intensity of the inner-surface hydroxyl stretching bands and the appearance of new bands at 3658, 3531 and 3499  $\text{cm}^{-1}$  (A, B and C, respectively). These new



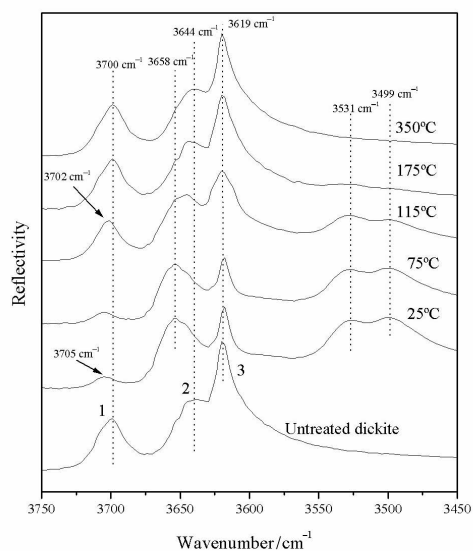


**Fig. 6** ATR-FTIR spectra of the 3750–3450  $\text{cm}^{-1}$  region of untreated dickite, and of the dickite–DMSO complex obtained at room temperature and after heating at increasing temperatures

bands were assigned by Olejnik *et al.* [1] to the H-bonding formed between the sulfonyl group of the DMSO molecules and the inner-surface hydroxyl groups. Similarly, Johnston *et al.* [6] assigned the 3531 and 3499  $\text{cm}^{-1}$  bands to stretching vibra-

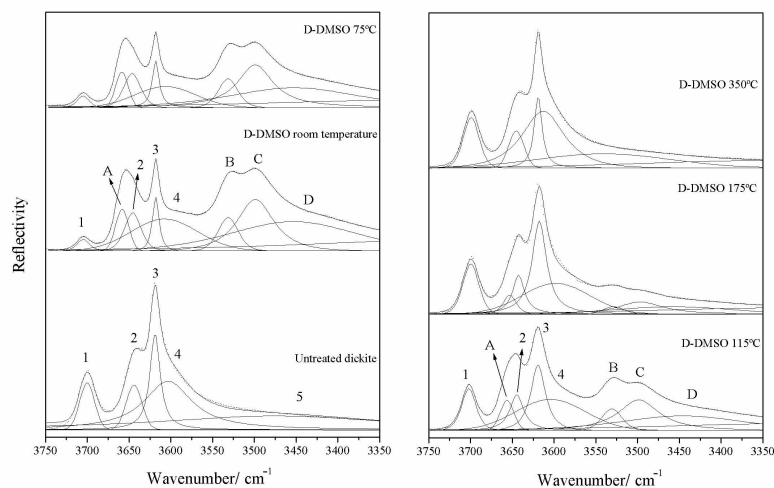


**Fig. 7** Band component analysis of the OH stretching region of the ATR-FTIR spectra of untreated dickite, and of the dickite–DMSO complex obtained at room temperature and after heating at increasing temperatures

tions of inner-surface hydroxyl groups bonded to DMSO molecules. Recently, a new interpretation of these bands, based on the assumption of the presence of water in the kaolinite–DMSO complex has been proposed by Frost *et al.* [8]. These authors assigned the  $3658\text{ cm}^{-1}$  band to the formation of a hydrogen bond between the inner-surface hydroxyls and the sulfonyl groups and the other two bands to water intercalated together with the DMSO.

Figure 7 shows the band component analysis of this region of the spectra. Areas, positions and bandwidths of the bands are summarised in Table 1. The asymmetry of the band 3 in the ATR-FTIR spectrum of the untreated dickite reveals the contribution of another band at slightly lower frequencies. This band has been previously observed in the FTIR spectra of nacrite [21], although it has not been interpreted. The curve-fitting analysis of the ATR-FTIR spectrum of the D-DMSO obtained at room temperature shows that the intercalation of DMSO molecules causes a general decrease in the intensity of both inner-surface and inner OH stretching bands of dickite (Table 1). This behaviour suggests that the inner hydroxyl groups are also perturbed by the DMSO intercalation due to the keying of a part of the DMSO molecule in the ditrigonal cavity [22]. Bands 1 and 2 correspond to the fraction of non-intercalated dickite, as indicated in the TG calculations and the degree of intercalation estimated from the XRD data.

Figure 8 shows the  $1750\text{--}1250\text{ cm}^{-1}$  region of the ATR-FTIR spectra of the DMSO liquid, the untreated dickite and the D-DMSO complex heated at increasing temperatures. This figure reveals that the DMSO liquid contains a certain amount of water indicated by the presence of a band at  $1654\text{ cm}^{-1}$  assigned to the water bending

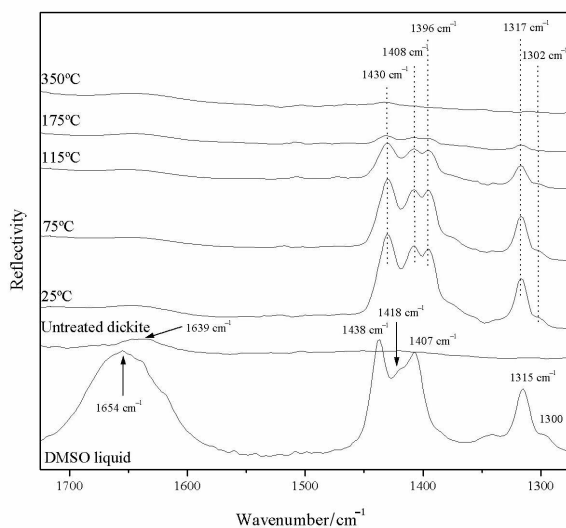


**Fig. 8** ATR-FTIR spectra of the  $1700\text{--}1300\text{ cm}^{-1}$  region of DMSO liquid, untreated dickite, and of the dickite–DMSO complex obtained at room temperature and after heating at increasing temperatures

**Table 1** Band positions, full width at half-maximum (FWHM) and band areas calculated from the ATR-FTIR of the hydroxyl stretching region of untreated dickite, dickite-DMSO obtained at room temperature and after heating at increasing temperatures

Untreated dickite				D-DMSO room temperature				D-DMSO 75°C			
Band	Center/ cm <sup>-1</sup>	FWHM/ cm <sup>-1</sup>	Area	Band	Center/ cm <sup>-1</sup>	FWHM/ cm <sup>-1</sup>	Area	Band	Center/ cm <sup>-1</sup>	FWHM/ cm <sup>-1</sup>	Area
1	3700	21.2	3.5	1	3704	17.2	0.73	1	3705	17.2	0.74
				A	3658	18.7	5.76	A	3658	17.9	4.80
2	3644	22.4	7.2	2	3645	22.8	3.22	2	3645	23.6	2.90
3	3618	14.8	14.7	3	3618	9.5	4.40	3	3618	9.8	4.19
4	3603	69.5	32.4	4	3607	92.2	20.19	4	3605	89.0	14.59
5	3475	335.9	35.9								
				B	3531	27.8	6.82	B	3531	26.9	5.82
				C	3498	58.3	34.46	C	3499	56.2	24.45
				D	3442	163.3	28.72	D	3438	158.2	21.00
D-DMSO 115°C				D-DMSO 175°C				D-DMSO 350°C			
Band	Center/ cm <sup>-1</sup>	FWHM/ cm <sup>-1</sup>	Area	Band	Center/ cm <sup>-1</sup>	FWHM/ cm <sup>-1</sup>	Area	Band	Center/ cm <sup>-1</sup>	FWHM/ cm <sup>-1</sup>	Area
1	3702	20.4	3.27	1	3699	22.5	4.20	1	3699	22.3	4.16
A	3656	19.3	4.16	A	3653	18.4	1.35				
2	3644	19.9	6.65	2	3642	17.2	6.73	2	3645	21.5	5.69
3	3619	20.7	11.72	3	3617	20.7	19.08	3	3619	11.2	7.90
4	3604	97.9	21.72	4	3597	95.4	20.92	4	3613	59.4	27.67
								5	3540	187.1	18.85
B	3530	28.3	4.51	B	3528	29.4	1.56				
C	3498	58.4	16.27	C	3496	63.5	7.56				
D	3446.3	174.6	19.41	D	3456.6	165.5	8.94				

mode [23]. The DMSO liquid also present, in this region of the spectra bands at 1438, 1418, 1407, 1315 and 1300  $\text{cm}^{-1}$ . These later bands were assigned to asymmetric  $\text{CH}_3$  deformation modes (1438, 1418, 1407  $\text{cm}^{-1}$ ) and to symmetric  $\text{CH}_3$  deformation modes (1315 and 1300  $\text{cm}^{-1}$ ) of DMSO molecules [24]. The untreated dickite, used as starting material, present, in the 1750–1250  $\text{cm}^{-1}$  region, a very small band at 1639  $\text{cm}^{-1}$  due to a negligible amount of water molecules which are usually adsorbed at the particle surface of natural materials. This band is hardly visible in the FTIR spectrum of the D-DMSO complex obtained at room temperature, indicating that water has been desorbed during the formation of the complex, since the sample was maintained, four weeks, at 50°C.

The series of spectra shown in Fig. 8 indicate that heating to 75°C causes a slight decrease in the intensity of the methyl deformation bands while the OH stretching bands of the complex remain practically unaffected at this temperature (Figs 6 and 7). This indicates that the DMSO lost below 75°C was adsorbed on the particle surface, since a partial deintercalation should modify the intensity and the wavenumber of the bands observed in the OH stretching region. On the other hand, at 115°C, the intensities of the methyl deformation bands decrease (Fig. 8) whereas band 1 intensifies and shifts from 3705 to 3702  $\text{cm}^{-1}$  (Figs 6 and 7). Concomitantly, the maximum of the 3658  $\text{cm}^{-1}$  band (Fig. 6) is shifted to lower frequencies as a consequence of the partial regeneration of the 3644  $\text{cm}^{-1}$  band of dickite (Figs 6 and 7), and the bands at 3531 and 3499  $\text{cm}^{-1}$  decrease in intensity. The behaviour of these bands suggests that the elimination of intercalated molecules begins after heating above 75°C.

A new decrease in the intensities of the methyl deformation bands is evident in the spectrum obtained at 175°C (Fig. 8). This decrease is, again, accompanied by an increase in the intensity of the bands 1 and 2, and the drastic decrease of the bands A, B and C (Figs 6 and 7).

The spectrum obtained after heating at 350°C reveals the loss of the DMSO bands and the regeneration of the hydroxyl stretching bands of dickite (Figs 6 and 7).

## Discussion

To correctly interpret the HTXRD and the DTA-TG data, the question of the possible presence of water molecules in the intercalate, as proposed by Frost *et al.* [8–10] in the case of the K-DMSO complex, must be considered. As indicated by Franco & Ruiz Cruz [11], it is difficult to prove the presence or absence of water in the intercalate, even using spectroscopic methods because it is usually present in the spectra of clay minerals obtained in ambient conditions. Nevertheless, this water band is hardly visible in the spectrum of the D-DMSO complex obtained at room temperature (Fig. 8) and it is not present in the spectrum of the complex, obtained after heating at 75°C, when the adsorbed material was eliminated. Consequently, we consider that water, if is present, is in a negligible amount and it is adsorbed at the external particle surface of the complex.

In order to compare the results obtained from the different techniques used in this work, we have to take in mind the different thermal regimes used in each one of

them. The heating regime used for the HTXRD study was a discontinuous heating rate, whereas for the ATD-TG analysis the heating rate was continuous. On the other hand, the heating regime of the ATR-FTIR study was firstly a continuous heating rate, until reaching the selected temperature, and then isothermic, since the sample was held at the selected temperature for 600 s. Under such conditions, beginning and final temperatures of the DMSO deintercalation process, determined with the different techniques, increases in this order: HTXRD < ATR-FTIR < ATD-TG.

In the first stage of heating (25–75°C), the ATR-FTIR spectra shows a slight decreasing of the methyl deformation bands which is not accompanied by modifications in the intensity of the bands observed in the OH stretching region. This results indicates that the bonding between OH groups and DMSO molecules are not affected by this first mass loss. For this reason, the mass loss between 25 and 75°C may be attributed to the loss of DMSO adsorbed on the particle surface of the complex. This loss is responsible for the endothermic effect centred at 57°C and represent 8% of the total adsorbed and intercalated molecules. The intensity of this endothermic effect and the mass loss are smaller than those observed in the DTA and TG curves of K-DMSO complex [11], thus indicating that the mass of adsorbed molecules, per  $[\text{Si}_2\text{Al}_2\text{O}_5(\text{OH})_4]$  unit, in D-DMSO complex is lesser than that observed in K-DMSO. This behaviour can be related to the particle-size, which is notably higher in dickite than in kaolinite. In this first stage of heating (25–70°C) the HTXRD patterns shows a decreasing of the 11-Å reflection of the complex, which indicates that, in a discontinuous heating rate, the DMSO deintercalation occurs at lower temperatures. It is possible that the deintercalation process begins when all the adsorbed molecules have been eliminated.

The ATR-FTIR data indicate that heating above 75°C causes the elimination of the intercalated molecules. The DTA curve shows that from this temperature the DMSO elimination occurred, at least, through two stages as revealed by the presence of two endothermic effect centred at 98 and 212°C. The HTXRD patterns obtained above 70°C revealed, at 80°C, a dilation of the structure (from 11.04 to 11.15 Å), which is followed, at 90°C, by a slight contraction at the same time that the reflection decreases in intensity. This contraction may be related to the loss between of the 6.5% of the intercalated molecules which would cause a different arrangement of the DMSO molecules in the interlayer space of dickite, as observed Raupach *et al.* [25]. This rearrangement of DMSO molecules causes the loss of the three dimensional ordering of the complex as revealed the XRD pattern obtained at 90°C. The endothermic effect centred at 98°C reflects these changes.

Some differences in thermal behaviour between D-DMSO and K-DMSO are observed above 90°C. The complete loss of the 11-Å reflection of K-DMSO complex occurred at 100°C [11] whereas the loss of the 11-Å reflection of the D-DMSO complex occurred at 175°C. Thus, the thermal stability of the D-DMSO complex appears to be higher than that of the K-DMSO complex. The complete loss of the basal reflection of the D-DMSO complex, above 150°C, without restoration of the 7-Å dickite reflection indicates that the dickite forms now a single layer complex [11]. Thus, the  $c^*$ -ordering of the

D-DMSO complex is only possible when the ratio  $[\text{Si}_2\text{Al}_2\text{O}_5(\text{OH})_4]:[(\text{CH}_3)_2\text{SO}]$  in intercalated particles is higher than 1:0.9.

The rearrangement of dickite layers is revealed by the total restoration of the dickite reflections at 300°C, where the TG curve indicates that the loss of the intercalated species has been completed. It is also reflected in the DTA curve, by the presence of an endothermic effect at 318°C.

The HTXRD patterns obtained in the 300–600°C range (Fig. 5) revealed a gradual decrease in intensity of the dickite reflection. This range agrees with the temperatures of dehydroxylation of dickite, which occurs in a narrower interval compared to untreated dickite due to the structural modifications induced in dickite by the intercalation–deintercalation processes.

### Concluding remarks

The HTXRD patterns and the DTA-TG curves of the dickite-DMSO intercalation complex indicate that there are differences in the thermal stability of the complexes formed with kaolinite and dickite.

Removal of adsorbed and intercalated molecules from the D-DMSO complex occurs in several stages, which are similar to those observed during heating of the K-DMSO complex. Adsorbed molecules are lost below 75°C. Loss of ~6.5% of the intercalated DMSO first causes a slight contraction of the basal spacing at 90°C (from 11.15 to 11.09 Å), due to a rearrangement of the DMSO molecules in the interlayers positions. This contraction is followed by the formation of a single layer complex. The increase in intensity and sharpening of the dickite reflections occurs at 300°C, when the loss of the intercalated species has been completed.

XRD data indicate an increase of disorder in the deintercalated dickite, which is also reflected in the position and shape of the endothermic effect due to dehydroxylation in the DTA curve.

Infrared spectra indicate that the amount of water present in the D-DMSO complex is negligible and it is mainly adsorbed on the particle surface. No evidence of intercalated water has been found in this study.

\* \* \*

The authors are grateful to S. Yariv, I. Lapides and to the unknown referee for carefully reviewing this paper and making helpful comments. This study has received financial support from the Research Group RNM-0199 (Junta de Andalucía).

### References

- 1 S. Olejnik, L. A. G. Aylmore, A. M. Posner and J. P. Quirk, *J. Phys. Chem.*, 72 (1968) 241.
- 2 S. González García and M. Sánchez Camazano, *An. Edaf. Agrob.*, 24 (1965) 495.
- 3 H. Jacobs and M. Sterctx, M., In: J. M. Serratosa (Ed.), *Proc. Reunion Hispano-Belga de Minerales de la Arcilla, C.S.I.C., Madrid 1970*, p. 154.
- 4 O. Anton and P. G. Rouxhet, *Clays Clay Miner.*, 25 (1977) 259.

- 5 J. M. Adams and G. Wautl, *Clays Clay Miner.*, 28 (1980) 130.
- 6 C. T. Johnston, G. Sposito, D. F. Bocian and R. R. Birge, *J. Phys. Chem.*, 88 (1984) 5959.
- 7 J. G. Thompson and C. Cuff, *Clays Clay Miner.*, 33 (1985) 490.
- 8 R. L. Frost, J. Kristóf, G. N. Paroz and J. T. Kloprogge, *J. Phys. Chem. B*, 102 (1998) 8519.
- 9 R. L. Frost, J. Kristóf, E. Horvath and J. T. Kloprogge, *Thermochim. Acta*, 327 (1999) 155.
- 10 R. L. Frost, J. Kristóf, E. Horvath and J. T. Kloprogge, *J. Phys. Chem. A*, 48 (1999) 9654.
- 11 F. Franco and M. D. Ruiz Cruz, *Clays Clay Miner.*, 50 (2002) 46.
- 12 M. Zamama, A. Burneau and R. Mokhlisse, *Spectrochim. Acta A*, 51 (1995) 101.
- 13 M. D. Ruiz Cruz and F. Franco, *Clays Clay Miner.*, 48 (2000) 63.
- 14 M. D. Ruiz Cruz and F. Franco, *Clays Clay Miner.*, 48 (2000) 586.
- 15 M. D. Ruiz Cruz and E. Reyes, *Appl. Geochem.*, 13 (1998) 95.
- 16 R. L. Frost and A. M. Vassallo, *Clays Clay Miner.*, 44 (1996) 635.
- 17 L. Stoch, *J. Therm. Anal.*, 29 (1984) 919.
- 18 B. D. Cullity, *Diffraction I: The directions of diffracted beams*. In: *Elements of X-ray diffraction*, Addison-Wesley Publishing Co., USA 1956, pp. 78–103.
- 19 G. W. Brindley, K. Chich-Chgun, J. L. Harrison, M. L. Lipsicas and R. Raythata, *Clays Clay Miner.*, 34 (1986) 239.
- 20 V. C. Farmer, *Spectrochim. Acta A*, 56 (2000) 927.
- 21 S. Shoval, S. Yariv, K. H. Michaelian, M. Boudeulle and G. Panczer, *Optical Mater.*, 16 (2001) 311.
- 22 S. Yariv, I. Lapidés, A. Nasser, N. Lahav, I. Brodsky and K. H. Michaelian, *Clays Clay Miner.*, 48 (2000) 10.
- 23 V. C. Farmer, *The common chain, ribbon, and ring silicates*. In: V. C. Farmer (Ed.), *Infrared spectra of minerals*. Mineral. Soc., London 1974, pp. 307–308.
- 24 W. D. Horrocks and F. A. Cotton, *Spectrochim. Acta.*, 17 (1961) 134.
- 25 M. Raupach, P. F. Barron and J. G. Thompson, *Clays Clay Miner.*, 35 (1987) 208.